European Spine Journal
https://doi.org/10.1007/s00586-024-08153-5

ORIGINAL ARTICLE

Lateral fenestration of lumbar intervertebral discs in rabbits: development and characterisation of an in vivo preclinical model with multi-modal endpoint analysis

James D. Crowley[1] · Rema A. Oliver[1] · Tian Wang[1] · Matthew H. Pelletier[1] · William R. Walsh[1]

Received: 7 August 2023 / Revised: 19 December 2023 / Accepted: 21 January 2024

Abstract

Purpose To evaluate the biological and biomechanical effects of fenestration/microdiscectomy in an in vivo rabbit model, and in doing so, create a preclinical animal model of IVDD.

Methods Lateral lumbar IVD fenestration was performed in vivo as single- (L3/4; $n=12$) and multi-level (L2/3, L3/4, L4/5; $n=12$) fenestration in skeletally mature 6-month-old New Zealand White rabbits. Radiographic, micro-CT, micro-MRI, non-destructive robotic range of motion, and histological evaluations were performed 6- and 12-weeks postoperatively. Independent t tests, one-way and two-way ANOVA and Kruskal–Wallis tests were used for parametric and nonparametric data, respectively. Statistical significance was set at $P<0.05$.

Results All rabbits recovered uneventfully from surgery and ambulated normally. Radiographs and micro-CT demonstrated marked reactive proliferative osseous changes and endplate sclerosis at fenestrated IVDs. Range of motion at the fenestrated disc space was significantly reduced compared to intact controls at 6- and 12-weeks postoperatively ($P<0.05$). Mean disc height index percentage for fenestrated IVDs was significantly lower than adjacent, non-operated IVDs for both single and multi-level groups, at 6 and 12 weeks ($P<0.001$). Pfirrmann MRI IVDD and histological grading scores were significantly higher for fenestrated IVDs compared to non-operated adjacent and age-matched control IVDs for single and multi-level groups at 6 and 12 weeks ($P<0.001$).

Conclusions Fenestration, akin to microdiscectomy, demonstrated significant biological, and biomechanical effects in this in vivo rabbit model and warrants consideration by veterinary and human spine surgeons. This described model may be suitable for preclinical in vivo evaluation of therapeutic strategies for IVDD in veterinary and human patients.

Keywords Disc disease · Fenestration · Intervertebral disc · Intervertebral disc degeneration · Microdiscectomy, Preclinical · Spine · Spine research

Introduction

Intervertebral disc degeneration (IVDD) is common to dogs and humans and is an example of the concept of Zoobiquity; the sharing of knowledge between human and veterinary medicine and recognising the commonality of disease processes between species [1]. Hansen Type 1 IVDD, common in chondrodystrophic dog breeds, is characterised by chondroid metaplasia of the nucleus pulposus (NP) [1]. Extrusion of NP into the vertebral canal causes compression and/or contusion of the spinal cord and subsequent neurological dysfunction. Fenestration is the surgical removal of the NP via annulotomy and is described as a prophylactic procedure to limit recurrence of IVD extrusion (IVDE) [2, 3]. In humans, fenestration is akin to microdiscectomy; the most common spinal surgical procedure for symptomatic lumbar disc herniation [4].

Fenestration of the herniated disc space at the time of spinal cord decompression is recommended to prevent, in the early postoperative period, continued extrusion of degenerate disc material, which may result in early recurrence of clinical signs [5, 6]. Although fenestration does not purport to reduce the compression on the spinal cord that

✉ James D. Crowley
james.crowley@unsw.edu.au

[1] Surgical and Orthopaedic Research Laboratories (SORL), Prince of Wales Clinical School, Faculty of Medicine, University of New South Wales (UNSW) Sydney, Prince of Wales Hospital, Sydney, NSW, Australia

Published online: 19 February 2024

results from the extruded disc, it is thought to reduce the risk of further extrusions from an already damaged annulus [5, 7–9], thus preventing worsening of clinical signs. Fenestration is also performed by some veterinary surgeons as a prophylactic measure, whereby adjacent non-extruded disc spaces are fenestrated to prevent future extrusion. Several large-scale retrospectives, and two prospective studies have evaluated the effect of fenestration on recurrence of IVDE in dogs [5–10]. Multiple veterinary studies strongly support the prophylactic effect of fenestration in dogs with previous episodes of symptomatic IVDE [5, 7, 9]. Published information suggests recurrence rates of 0% to 24.4% with prophylactic disc fenestration [11–16] and 2.67% to 41.7% without prophylactic disc fenestration [13, 16–21]. Arguably the most reliable body of work we have in support of the protective effect of fenestration on future occurrence of IVDE is the randomised prospective clinical trial by Brisson et al. (2011). The authors aimed to determine if multiple-site disc fenestration decreased the incidence of recurrent IVDE, compared with single-site disc fenestration, in small-breed dogs treated for IVDE. The authors concluded that dogs undergoing single-site disc fenestration only at the site of extrusion at the time of decompressive surgery were significantly more likely to develop subsequent thoracolumbar IVDE (17.89% [17/95]) than dogs that underwent multiple-site disc fenestration from T11 through L4 (7.45% [7/94]) [5]. From this difference of approximately 10%, as posed by Jeffery and Freeman (2018) [2], a more difficult, philosophic, question centres on whether it is appropriate to treat a certain number of dogs to prevent a much smaller number from developing recurrence. Furthering our understanding on the biological and biomechanical effects of fenestration would help to answer this question.

In humans, an annulotomy for the surgical removal of herniated disc material, termed microdiscectomy, is considered the gold standard for treatment of most lumbar IVD herniations. The less invasive approach, and better visualisation of the surgical field is preferred over a standard open discectomy [22]. Complications from microdiscectomy include iatrogenic injuries such as durotomy, nerve root injury or instability, recurrent disc herniations, haematoma, infection, and persistent pain. One large case series of 2500 microdiscectomy patients reported a complication rate of less than 1.5% [23]; however, like fenestration in veterinary medicine, there is a lack of data on the biological and biomechanical implications of microdiscectomy on the IVD.

Preclinical animal models, including rat, rabbit, dog, and many other species, have been documented extensively in the literature to investigate the performance of biological and biomechanical materials and evaluate treatment strategies for a myriad of disease processes in veterinary and human medicine [24]. There is a paucity of veterinary and human literature describing the biological and biomechanical implications of fenestration and microdiscectomy. There is a need for preclinical surgical models of IVD fenestration, to further define the biological and biomechanical consequences of the procedure. Therefore, the objectives of this study were to (1) characterise the biological and biomechanical impact of lateral lumbar IVD fenestration in a preclinical in vivo rabbit model as a model for the canine scenario and in doing so, (2) create a suitable preclinical animal model for IVDD in humans. We hypothesised that there would be a significant difference between fenestrated and control rabbit lumbar IVDs regarding (1) disc height index as assessed on lumbar radiographs, (2) Pfirrmann IVDD scoring on MRI scans, (3) biomechanical range of motion (ROM) testing, and (4) histological grading of IVDD. This research hypothesis was tested against a null hypothesis of no difference for all endpoints.

Methods

In vitro lumbar IVD fenestration

The surgical technique of lateral lumbar IVD fenestration (L2/3, L3/4, L4/5) was developed using skeletally mature 6-month-old New Zealand White (NZW) rabbit cadavers ($n=6$) weighing 3.5–4.5 kg (Fig. 1). Lumbar discs spaces were chosen due to the authors' familiarity with the surgical anatomy and in accordance with preclinical in vivo rabbit models of IVDD [25]. Briefly, a left lateral approach to each lumbar disc was performed by a muscle splitting approach through the transverse abdominis, external abdominal oblique and internal abdominal oblique muscles. Next, the psoas muscle was retracted ventrally from the vertebral transverse process(es) to expose the IVD. Fenestration was performed by making a 1.5×2 mm window in the lateral annulus fibrosus (AF) with a no. 11 scalpel blade to remove the NP with a spinal curette. The aim was to remove as much NP tissue as possible as per the intention of the technique in canine literature to prevent future IVDE. The soft tissues were closed routinely.

In vivo lumbar IVD fenestration

The surgical technique was extrapolated to the in vivo setting. The in vivo study was approved by the Animal Care and Ethics Committee (#20/90A) at the University of New South Wales, Sydney, Australia. Preoperative animal preparation included a clinical veterinary examination as well as routine haematology and biochemistry blood work to confirm animal status. Skeletal maturity of each rabbit was verified by radiographic confirmation of growth plate closure at the proximal tibia [26]. Single-level (L3/4; $n=12$) and multi-level (L2/3, L3/4, L4/5; $n=12$) fenestration was

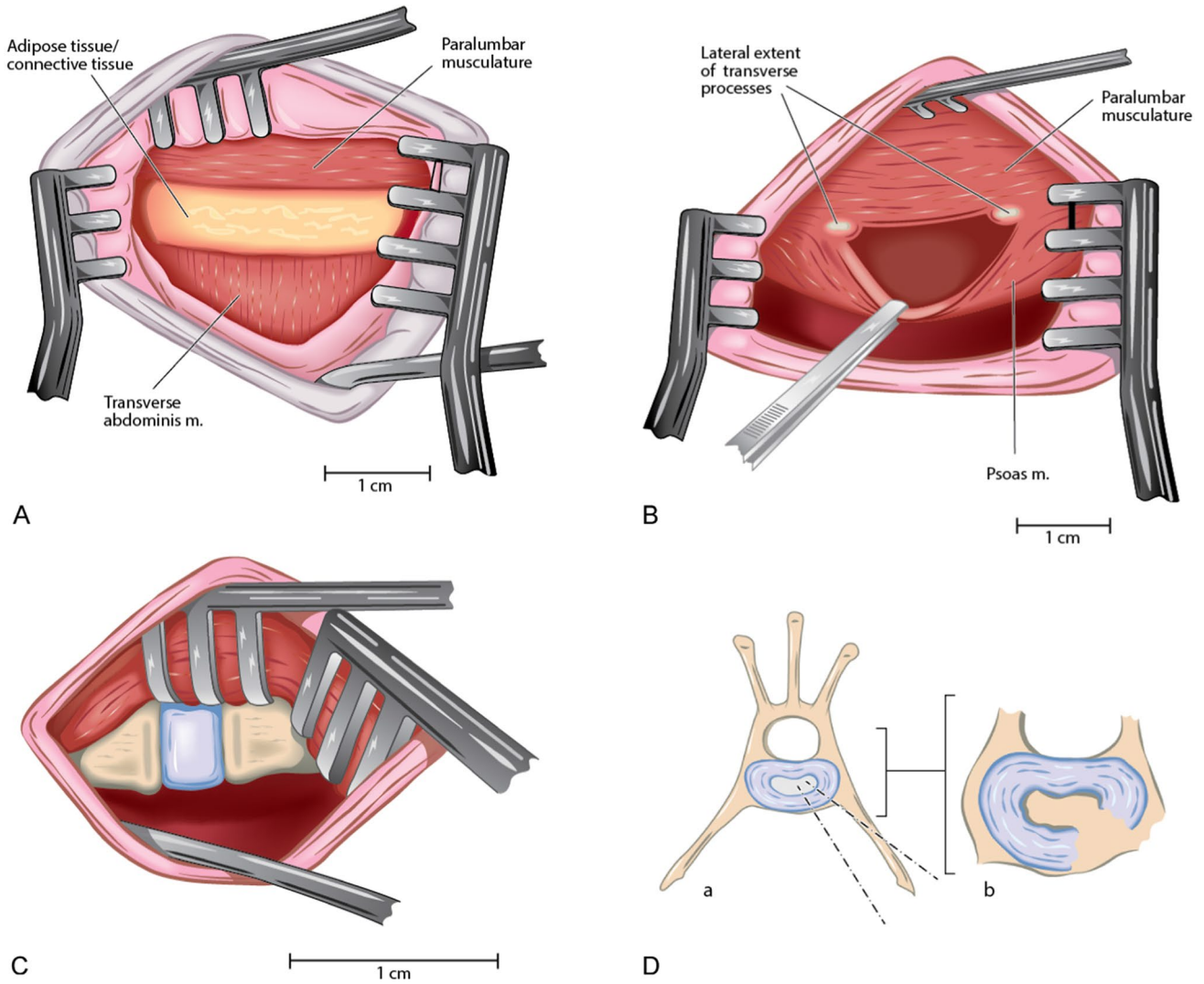

Fig. 1 (**A**–**D**). Schematic illustration of the step-wise surgical approach for left lateral lumbar IVD fenestration in a rabbit model. A left lateral approach to each lumbar disc was performed via a muscle splitting technique (**A**), reflecting the psoas muscle ventrally (**B**) to expose the disc space for fenestration (**C**). Note the annular window (a) and working angle of fenestration (b) in the rabbit due to the cranioventral angulation of the transverse processes

performed in skeletally mature, 6-month-old, female entire NZW rabbits ($n = 24$ total) as described above. The surgeon made a 1.5×2 mm window in the left lateral annulus and removed as much nucleus pulposus as was reasonably possible, as described above. Rabbits were randomly allocated to 6- and 12-week timepoints ($n = 6$ per group per timepoint). The rabbits were premedicated with Buprenorphine (0.03 mg/kg) and Midazolam (0.5 mg/kg) via intramuscular injection using a 23 g needle. The rabbits were preoxygenated for 10 min prior to masked isoflurane induction and maintained to effect. A balanced crystalloid solution (Hartmann's solution) was administered subcutaneously (20 mL/kg) prior to commencement of surgery. Continuous multiparameter cardiopulmonary monitoring (Datalys V7, Lutech, Ronkonkoma, New York) was used throughout anaesthesia. The rabbits received external heat support in the form of a heat pad. Following completion of surgery, the rabbits were wrapped in a clean towel for added warmth and received masked oxygen supplementation until righting before being returned to their housing pen. All rabbits received perioperative prophylactic antibiotics (Procaine Penicillin 50 000 IU/KG IM), perioperative and intraoperative opioid analgesia (Buprenorphine 0.03 mg/kg IM at induction then as required), and postoperative nonsteroidal anti-inflammatory medication (Meloxicam 0.85 mg/kg q 12–24 h for 3–5 days). The rabbits were physically examined and weighed daily for the first week postoperatively then weekly until their timepoint by a veterinarian. Rabbits were group-housed in 3–3.2m^2 enclosed, hay-lined pens with no exercise restriction [26].

Harvest

The rabbits were euthanised via intracardiac injection of pentobarbitone under a deep plane of general anaesthesia. All major organs (heart, lungs, kidneys, spleen, and liver) were harvested, assessed for gross pathology and processed for paraffin histology. The surgical sites were closely examined, with the presence of gross inflammation, fibrous tissue, haematoma(s), and/or any other pathology recorded if present.

Radiographs

Preoperative and post-euthanasia lateral and dorsoventral lumbar spinal radiographs were performed. Radiographs of harvested lumbar spines were obtained using a high-resolution Faxitron X-ray machine and digital plates (AGFA CR MD4.0 Cassette). The digital images were processed using an AGFA Digital Developer and workstation (AGFA CR 75.0 Digitiser Musica, AGFA, Germany). Cull radiographs were examined for osseous changes such as osteophytosis, and disc space narrowing relative to the preoperative state.

Intervertebral disc height was expressed as disc height index (DHI), which was calculated based on a modified version of the method described by Lu et al. (1997) [27]. DHI was calculated as a ratio of the average dorsal, middle, and ventral IVD space measurements to the average of the dorsal, middle, and ventral vertebral body heights of the vertebral body cranial to the IVD space (Fig. 2). The average percentage change in DHI of all fenestrated and non-operated discs was calculated for each fenestrated disc as a ratio to its preoperative DHI [%DHI = (postoperative DHI/ preoperative DHI) × 100]. All radiographs were assessed by a single observer blinded to the animal's group and timepoint.

Magnetic resonance imaging (MRI)

Immediately following euthanasia, the lumbar spines were harvested and packaged for MRI scanning. Scans were performed using a 9.4-T Bruker BioSpec 94/20 Advance III micro- imaging MRI system (μMRI; Bruker, Ettlingen, Germany). The system was equipped with BGA-12S HP gradients with maximum strength 660 mT/m and slew rate 4570 Tm/s and a 50-mm quadrature radiofrequency volume transmit-receive coil. A 2D T2-weighted fast spin echo (FSE) sequence was optimised for the purpose and used to acquire 11 high-resolution image slices in sagittal orientation. The following basic protocol parameters were used for image acquisition: TR 2200 ms, TE 21 ms, ETL 4, 1 mm slices, with a FOV 80 × 40 mm, and R-P matrix size of 400 × 200 resulting in an in-plane resolution of 200 × 200 mm with a total acquisition time of 28 min.

The MRI degeneration grade of IVDs was classified according to the Pfirrmann grade using T2 weighted sagittal images [28]. The grading system was based on 4 criteria (signal intensity, disc structure, disc height, and distinction between the NP and AF). Pfirrmann scores ranged from grade 1 (healthy IVD) to 5 (end-stage IVD degeneration). This was performed for all fenestrated and non-operated adjacent IVDs in all 24 rabbits that underwent lumbar IVD fenestration as well as 6 control rabbit lumbar spines harvested from other ethically approved studies at

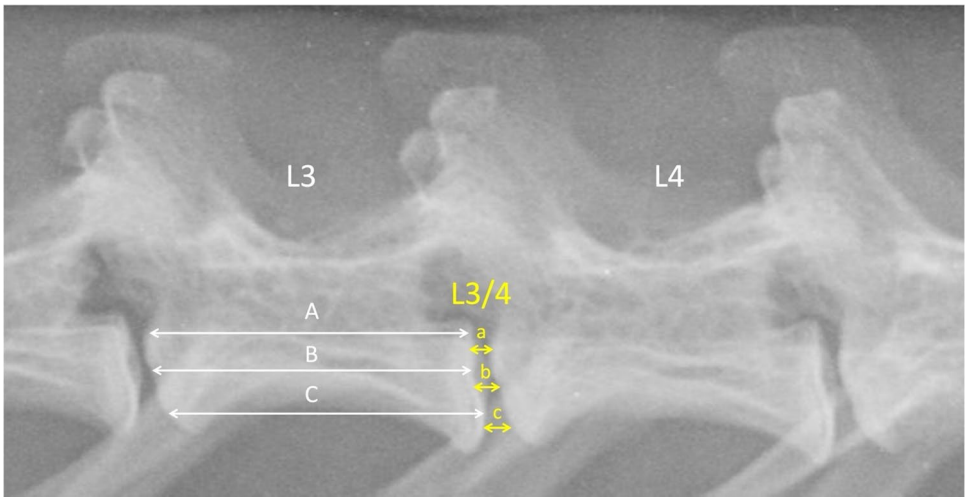

Fig. 2 Preoperative lateral radiograph of the L3 and L4 vertebrae and L3/4 intervertebral disc space. Disc height index (DHI) was calculated as a ratio of the average dorsal (a), middle (b), and ventral (c) IVD space measurements to the average of the dorsal (A), middle (B), and ventral (C) vertebral body heights of the vertebral body cranial to the IVD space. The average percentage change in DHI of all fenestrated and non-operated discs was calculated for each fenestrated disc as a ratio to its preoperative DHI [%DHI = (postoperative DHI/ preoperative DHI) × 100]

our institution. The evaluation was performed by a single observer blinded to the group and timepoint, and in random order.

Micro-computed tomography

Micro-computed tomography (μCT) was performed immediately following MRI on the intact samples prior to dissection to obtain high-resolution radiographic images of the fenestrated disc spaces and associated vertebral structures. μCT scans were performed in the sagittal plane using an Inveon Scanner (Siemens, USA). Scan effective pixel size or resolution was set to 54 μm for all scans. μCT scans were stored in DICOM format. The DICOM images were viewed using Inveon™ Research Workplace (IRW) (Siemens Medical Solutions, Knoxville, TN, USA). Three-dimensional models were reconstructed and examined in the transverse, sagittal, and coronal planes for any evidence of adverse osseous reactions, endplate sclerosis, and changes in IVD morphology.

Biomechanical testing

Non-destructive ROM testing was performed for the single-level group ($n = 12$) at 6- and 12-week timepoints. Spinal motion segments of the fenestrated disc space (L3/4) were dissected and tested with pure moments using a Denso robot (DENSO Corporation, Kariya, Aichi, Japan) to avoid off axis moments and spurious loading. After fixing the spines in custom moulds with resin, a three-dimensional coordinate system was established, and the specimens evaluated in axial rotation (AR), flexion–extension (FE), and lateral bending (LB). Moments of 300 *N*mm were applied at a rate of 33.3 *N*mm per second and held for 15 s [29]. A total of 4.5 load–unload cycles were run in each profile with the last three cycles analysed at 270 *N*mm and the mean of these three cycles reported. To provide a comparison to normal rabbit lumbar IVDs, ROM testing was performed on intact, non-operated L3/4 spinal motion segments from skeletally mature, age-matched female NZW rabbits ($n = 6$) that were euthanised as part of other ethically approved projects at our institution. ROM and neutral zone (NZ) was calculated using a custom MatLab script.

Histology

All specimens were fixed in phosphate-buffered formalin solution for a minimum of 48 h and decalcified in 10% formic acid–phosphate-buffered formalin solution for routine paraffin histology. Each specimen was sectioned into four blocks in the sagittal plane, so that the cranial endplate, IVD and caudal endplate were localised for each disc space. Each IVD was macroscopically assessed, paying attention to gross appearance, tissue architecture, and presence of fibrous tissue. The blocks (~ 3 mm in thickness) were embedded in paraffin and sectioned (5 microns) using a Leica Microtome (Leica Microsystems Pty Ltd, North Ryde, Australia). A minimum of three sections were cut from each paraffin block and stained with hematoxylin and eosin (H&E). Stained sections were examined in a blinded fashion (to treatment groups and timepoints) using an Olympus light microscope (Olympus, Japan) with a DP72 high-resolution video camera (Olympus, Japan). Eighteen discs from the six control rabbits used for mechanical testing were also evaluated. The stained sections were graded by a single observer blinded to rabbit ID, group and timepoint, using the recently established standardised histopathology scoring system of rabbit IVD degeneration (Fig. 3) [30]. Briefly, a three-category grading scheme (grade 0–2) across seven evaluated categories was used: NP morphology (shape and area), NP matrix condensation, NP cellularity, AF/NP border appearance, AF morphology, and endplate (EP) sclerosis/thickening. The total histological score (0–14) was calculated by summing grades across all categories, with greater scores indicating greater degeneration. Paraffin blocks from animals in each group and timepoint ($n = 1$ per treatment group per timepoint and $n = 1$ adjacent control disc) were selected for additional staining with Safranin-O (SO) and Picrosirius Red (PR) for qualitative analysis.

Statistical analysis

Sample size was based on a priori power assessment with power set at 0.8 and an alpha of 0.05, to provide the minimum number of animals to achieve the experimental endpoints. Descriptive data were presented as mean ± standard error. Statistical differences in DHI% between fenestrated and adjacent non- operated control IVDs was evaluated with a one-way ANOVA and Tukey post hoc test. Non-parametric Pfirrmann MRI and histological grading scores fenestrated and non-operated control samples were assessed with a Kruskal–Wallis test and Tukey post hoc. Biomechanical ROM for single-level L3/4 fenestration and age-matched control specimens was compared with a two-way ANOVA with post hoc Tukey test. Statistical analysis was performed using SPSS for Windows (SPSS, Chicago, IL). For all analyses, statistical significance was set at $P < 0.05$.

Results

The surgical technique of lateral fenestration of lumbar IVDs was developed in vitro and successfully extrapolated to the in vivo setting. The procedure was well-tolerated by all rabbits, with all surviving the procedure and reaching their respective timepoints with progressive increase in weight at

Category	Features	Score	Description
NP monophology	NP shape	0	Oval shape
		1	Oval/round with mild distortion
		2	Irregular shape
	NP area	0	NP constitutes 40-50% of disc area
		1	Mild to moderate reduction in NP area
		2	Severe reduction in NP area
NP matrix	Matrix condensation	0	Normal gelatinous appearance
		1	Slight condensation of the extracellular matrix
		2	Moderate/severe condensation of the extracellular matrix
NP cellularity	Cell number	0	High cell density
		1	Medium cell density
		2	Low cell density
AF/NP border	Border appearance	0	Normal, clear distinction between NP and AF
		1	Minimally interrupted, loss of distinction between NP and AF
		2	No distinction between NP and AF
AF	AF morphology	0	Normal, pattern of fibrocartilage lamellae (u-shaped posteriorly and slightly convex anteriorly), without ruptured fibers and without serpentine appearance anywhere in AF
		1	Ruptured or serpentine fibers in less than 30% of AF, mild/moderate infolding
		2	Ruptured or serpentine fibers in more than 30% of AF, severe infolding
EP	EP sclerosis/thickening	0	Thin cartilage endplate with many adjacent vascular/marrow channels.
		1	Mild/moderate thickening of cartilage endplate and reduction in number of adjacent vascular/marrow channels
		2	Severe thickening of the cartilage endplate and reduction in number of adjacent vascular/marrow channels

Abbreviations: AF, annulus fibrosus; EP, end plate; NP, nucleus pulposus.

Fig. 3 Histological IVDD grading system used in this study, as described by Gullbrand et al. (2021) [30] for preclinical in vivo rabbit studies

weekly assessment. The lateral approach allowed for sufficient depth of the fenestration into the NP to ensure maximal NP was retrieved.

Surgical model

The left lateral trans-psoas approach facilitated good exposure of the lumbar IVD for fenestration. Mean surgical time was 30.8 ± 19 min and 41.5 ± 9.6 min for the single-level and multi-level fenestration groups, respectively. No intraoperative complications were experienced. One rabbit self-traumatised the surgical site that resulted in wound dehiscence that required primary closure under general anaesthesia 2 days postoperative, from which the rabbit recovered uneventfully. All rabbits made a smooth recovery from anaesthesia and surgery, returning to normal ambulation once the effect of anaesthetic medications had dissipated. All rabbits demonstrated normal ambulation that continued up until their respective timepoints.

All surgical wounds were well healed at the time of euthanasia. There was no evidence of infection at the surgical sites; however, there was obvious thickening and fibrosis of the subcutaneous and deep muscular tissues at the fenestrated sites. Haematology and biochemistry blood work was unremarkable prior to surgery as well as at the time of euthanasia for all animals. No gross and histopathological

abnormalities were noted in the distant organs (heart, lungs, kidneys, spleen, and liver).

Radiography

Dorsoventral and lateral radiographs demonstrated marked reactive, proliferative osseus changes at both 6- and 12-week timepoints for all treated levels including osteophyte formation. Mean DHI% for all fenestrated IVDs were significantly lower than adjacent, non-operated IVDs for both single and multi-level groups, at 6 and 12 weeks ($P < 0.001$) (Table 1).

Table 1 Disc height index percentage (DHI%) for single- and multi-level lumbar IVD fenestration at 6 and 12 weeks

Intervertebral Disc	Single-Level 6 weeks ($n=6$)	Single-Level 12 weeks ($n=6$)	Multi-Level 6 weeks ($n=6$)	Multi-Level 12 weeks ($n=6$)
L1/2	–	–	92.14 (2.69)	85.17 (4.44)
L2/3	97.09 (4.34)	98.92 (5.58)	75.37 (2.52)**	67.05 (2.46)**
L3/4	53.37 (5.02)*	64.57 (5.58)*	70.69 (4.39)**	64.28 (2.46)**
L4/5	86.17 (2.96)	96.06 (2.99)	69.62 (4.43)**	62.10 (2.14)**
L5/6	–	–	85.32 (5.18)	80.10 (2.57)

Data are presented as mean (standard error)

*DHI% significantly lower than adjacent levels for single-level group; $P < 0.05$

**DHI% significantly lower than adjacent levels for multi-level group; $P < 0.05$

Micro-computed tomography

μCT images and 3D reconstructions at the 6- and 12-week endpoint for both single and multi-level groups are presented in Figs. 4 and 5. There was evidence of disc space narrowing, endplate sclerosis, and osteophytosis at the ventrolateral aspect of the fenestrated IVD space, and vertebral body, as well as the transverse processes for all operated rabbits.

Magnetic resonance imaging (MRI)

Representative sagittal T2 sequences for both single and multi-level groups for 6- and 12-week timepoints and the control group are shown in Fig. 6. Pfirrmann scores for all in vivo and control IVDs are presented in Table 2. All non-operated control IVDs from age-matched controls were scored Grade 1. For non-operated adjacent IVDs for both groups at both timepoints, 46/48 were scored Grade 1, with 2/48 scored Grade 2. No fenestrated disc scored less than a Pfirrmann grade 3 in any group at any timepoint, with 40/48 assigned as Grade 4 or 5. The injured IVD showed qualitatively decreased disc height with no signs of herniation,

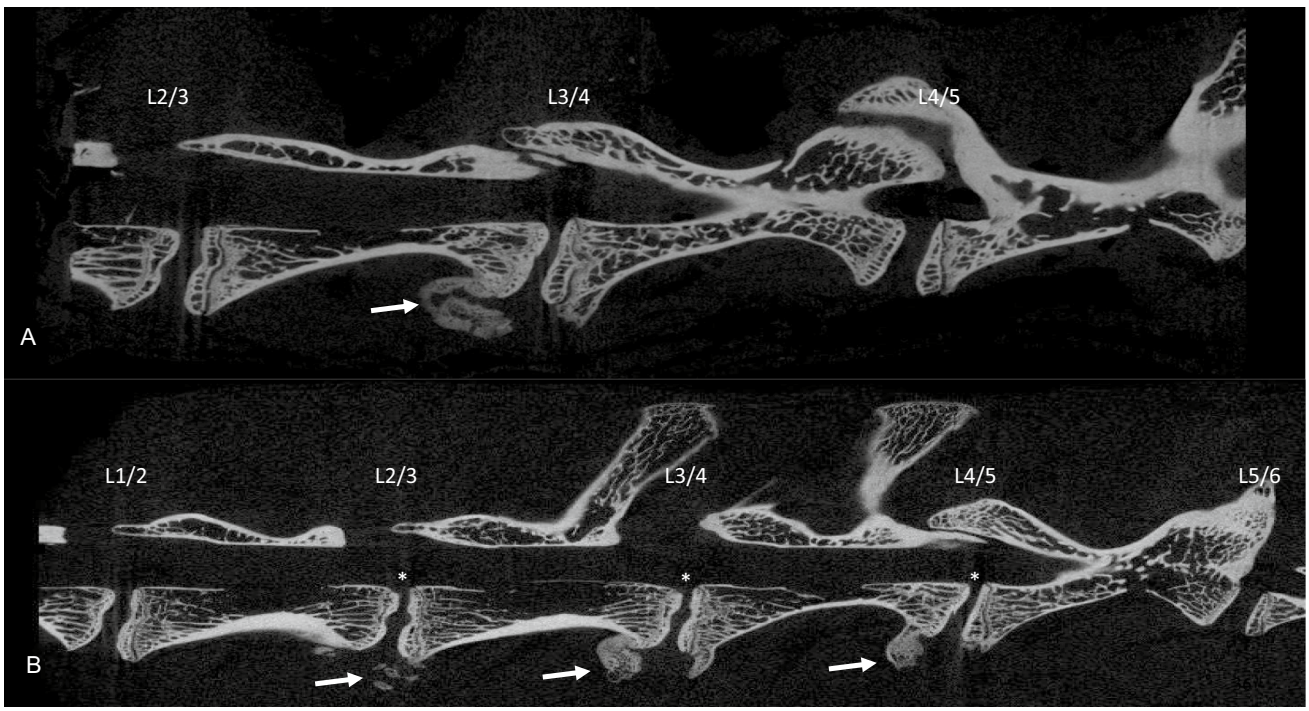

Fig. 4 Micro-CT images in the sagittal plane of single (**A**) and multi-level groups (**B**) at 6 weeks. Note disc space narrowing (*), osteophyte formation (white arrow), and endplate sclerosis for fenestrated IVDs (L3/4 and L2/3, L3/4, L4/5)

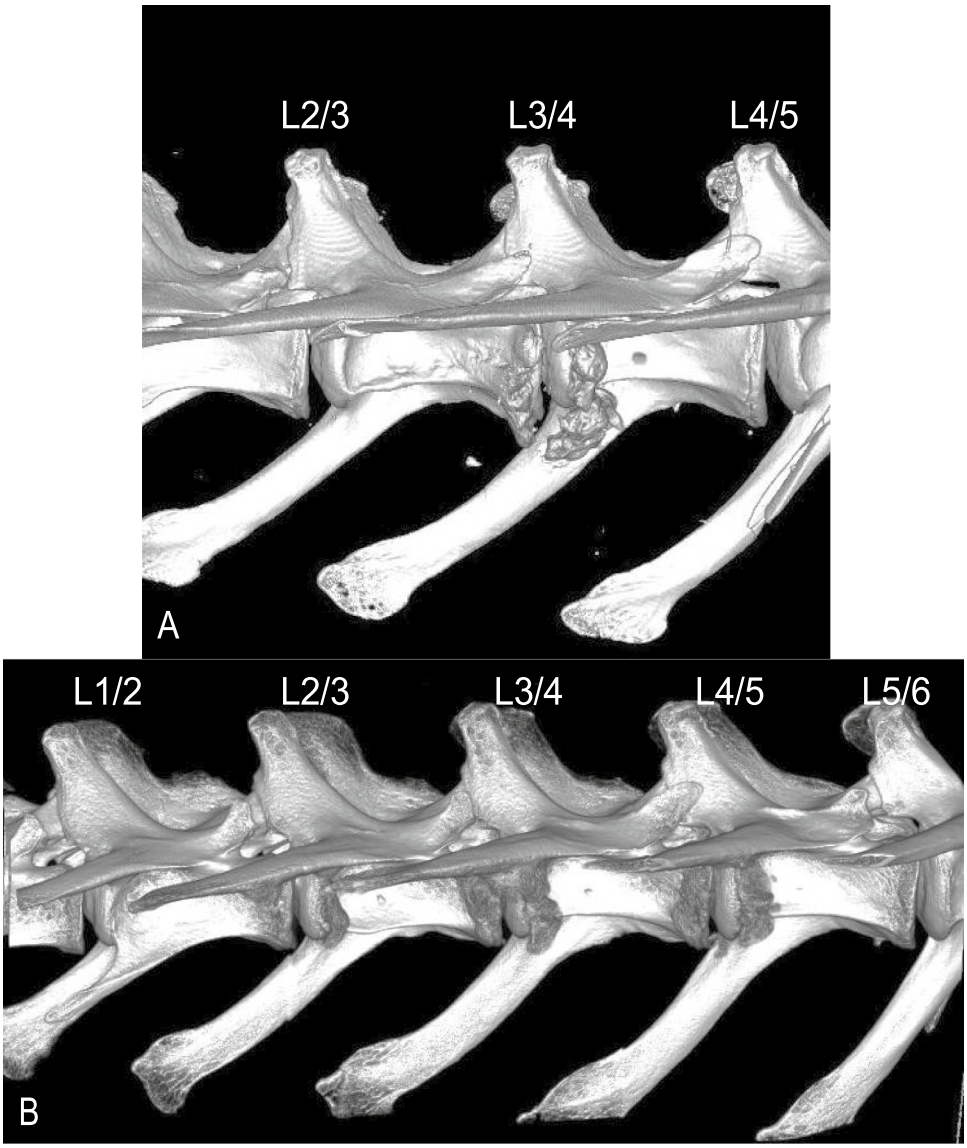

Fig. 5 Left lateral μCT 3D reconstructed images of a single (**A**) and multi-level fenestration (**B**) at 12 weeks, representative of the operative point of view. Note osteophyte formation on the ventral and left lateral aspect of the fenestrated disc spaces compared to the non-operated IVDs

protrusion, or extrusion. Fenestrated IVDs had a significantly higher Pfirrmann grade than both non-operated adjacent IVDs and non-operated controls ($P < 0.001$), while the median Pfirrmann score for adjacent disc spaces was not significant different from control IVDs.

Biomechanical testing

ROM and NZ analysis is presented in Table 3. Compared to non-operated controls, single-level fenestrated L3/4 motion segments had significantly reduced ROM and NZ in lateral bending at 6 ($P = 0.02$, $P = 0.02$) and 12 weeks ($P = 0.001$, $P = 0.001$) and flexion–extension at 6 ($P = 0.03$) and 12 weeks ($P = 0.002$, $P = 0.006$). In axial rotation, control spines had lower ROM and NZ than the operated animals at both timepoints; however, this was only significant for ROM at the 6-week timepoint ($P = 0.03$).

Macroscopic assessment of intervertebral discs

The condition of NP and AF tissue was assessed via macroscopic observation of freshly dissected IVD samples. For the non-operated adjacent and control IVDs, transparent, white, hydrated, fresh NP tissue was visible in the centre of the disc, almost oozing from within the disc space (Fig. 7A). The normal concentric lamellae structure of the AF was evident, clearly demarcating the boundary of the disc space and encapsulating the NP. For all fenestrated IVDs, the disc space was visibly collapsed with the majority of NP removed (Fig. 7B). The remaining tissue was degenerate, the AF structure was distorted, and the overall structure of the IVD was abnormal. There was significant fibrous tissue formation on the left lateral aspect of the annulus/intervertebral space (Fig. 7B, C). There were

palpable osseous thickening/proliferations at the lateral extremity of the transverse processes on the left-hand side.

Histology

Qualitatively, all fenestrated IVDs showed a combination of defects involving the AF and NP without signs of extrusion, along with degenerative and inflammatory changes. Fenestrated IVDs showed alterations in NP and AF morphology, blood vessel ingrowth, influx of mixed inflammatory cells and adherence of fibrous tissue, predominately on the left ventrolateral aspect of the disc space (Fig. 8B, C, E). Fenestrated IVDs scored at high severity for all evaluated categories, reflecting the structural changes of the AF and the NP, with distortion of the AF/NP boundary and the AF lamellar structure on the left ventral and lateral aspects.

There was evidence of endplate sclerosis at all operated IVDs. Blood vessel ingrowth was observed within the AF and into the NP to a lesser extent. There were increased populations of mixed mono and polymorphonuclear inflammatory cells (macrophages, lymphocytes, plasma cells and neutrophils), with interspersed moderately well organised fibrous connective tissue (fibroblasts), on the left lateral annulus, consistent with AF and NP injury and secondary biological response (Fig. 8B, C, E). There was also amorphous bone formation at this location, consistent with osteophytosis (Fig. 8C). In the adjacent non-operated and age-matched control groups, the NP tissue was well organised, resembling an oval shape and a clear boundary to AF (Fig. 8A). The NP matrix had a gelatinous appearance, with reduced cell density. Cartilaginous endplates were thin with many adjacent vascular channels. There was normal cell density within the NP.

Quantitative grading, where a higher score indicates a more degenerative disc, supported the above histological observations. The injured IVDs had statistically significant higher total histological scores than non-operated adjacent and age- matched control IVDs for both single and multiple groups at 6 and 12 weeks ($P < 0.001$) (Table 4). No significant difference was detected between non-operated adjacent and age-matched control IVDD scores in either group or timepoint. There was no significant effect of group or timepoint on histological scores. For adjacent non-operated control discs stained with SO, the nucleus stained intensively for proteoglycans. The endplates had a regular homogenous thickness and cartilage structure with chondrocytes embedded in a rich proteoglycan matrix, demonstrated by intense red staining (Fig. 9A, B). For fenestrated discs, there was marked reduction in red staining suggestive of reduced proteoglycan content albeit in a more collapsed disc space relative to the intact (Fig. 9C). Picrosirius staining demonstrated the normal concentric lamellar layers of collagen on the ventral aspect of the AF (Fig. 10A). In comparison, the disc space of fenestrated samples was collapsed, with disruption and loss of continuity of the normally well-arranged and aligned lamellar fibres suggestive of degeneration.

Discussion

The objectives of this study were to develop and characterise the biological and biomechanical impact of lateral lumbar IVD fenestration using an in vivo rabbit model and in doing so develop a preclinical model of IVDD in humans. We describe an in vivo preclinical rabbit model of lateral fenestration of lumbar IVDs that demonstrated the biological and biomechanical implications of this procedure. We hypothesised that there would be a significant difference between fenestrated and control rabbit lumbar IVDs regarding (1) disc height index as assessed on lumbar radiographs, (2) Pfirrmann IVDD scoring on μMRI scans, (3) biomechanical ROM testing, and (4) IVD histological grading of degeneration. This research hypothesis was tested against a null hypothesis of no difference for all endpoints. Compared to control IVDs, fenestrated IVDs for both single- and multi-level groups had significantly lower disc height indices, significantly increased Pfirrmann MRI grading scores, significantly reduced ROM (not evaluated in multi-site group), and significantly greater histological IVDD grading. Whilst there are inherent limitations in extrapolating results of preclinical models, the results of this experimental in vivo rabbit model are worthy of consideration by veterinary and human spine surgeons for the biological and biomechanical implications of fenestration and microdiscectomy, respectively. Additionally, the described technique may represent a suitable preclinical model of IVDD in humans that could be used to evaluate new treatment strategies, including NP augmentation.

A myriad of preclinical animal models of human IVDD have been described in the literature. Preclinical animal models provide measurable data on the biology, histopathology, pathophysiology, and biomechanics of IVDD that cannot be practically or ethically obtained from human patients [25, 31]. Preclinical IVDD animal models, both spontaneous and induced, allow for improvement in our understanding of the pathophysiology of IVDD and the preclinical evaluation of diagnostic, treatment, and preventative options [25]. The surgical technique of lateral fenestration of lumbar IVDs was developed in vitro and successfully extrapolated to the in vivo setting. The left lateral trans-psoas approach allowed for sufficient exposure and depth of fenestration. The procedure was well tolerated by all rabbits, with all animals surviving the procedure and reaching their respective timepoints. All rabbits were mobile from immediately following surgery and throughout the study period, including the absence of any neurological deficits. This may in part be due

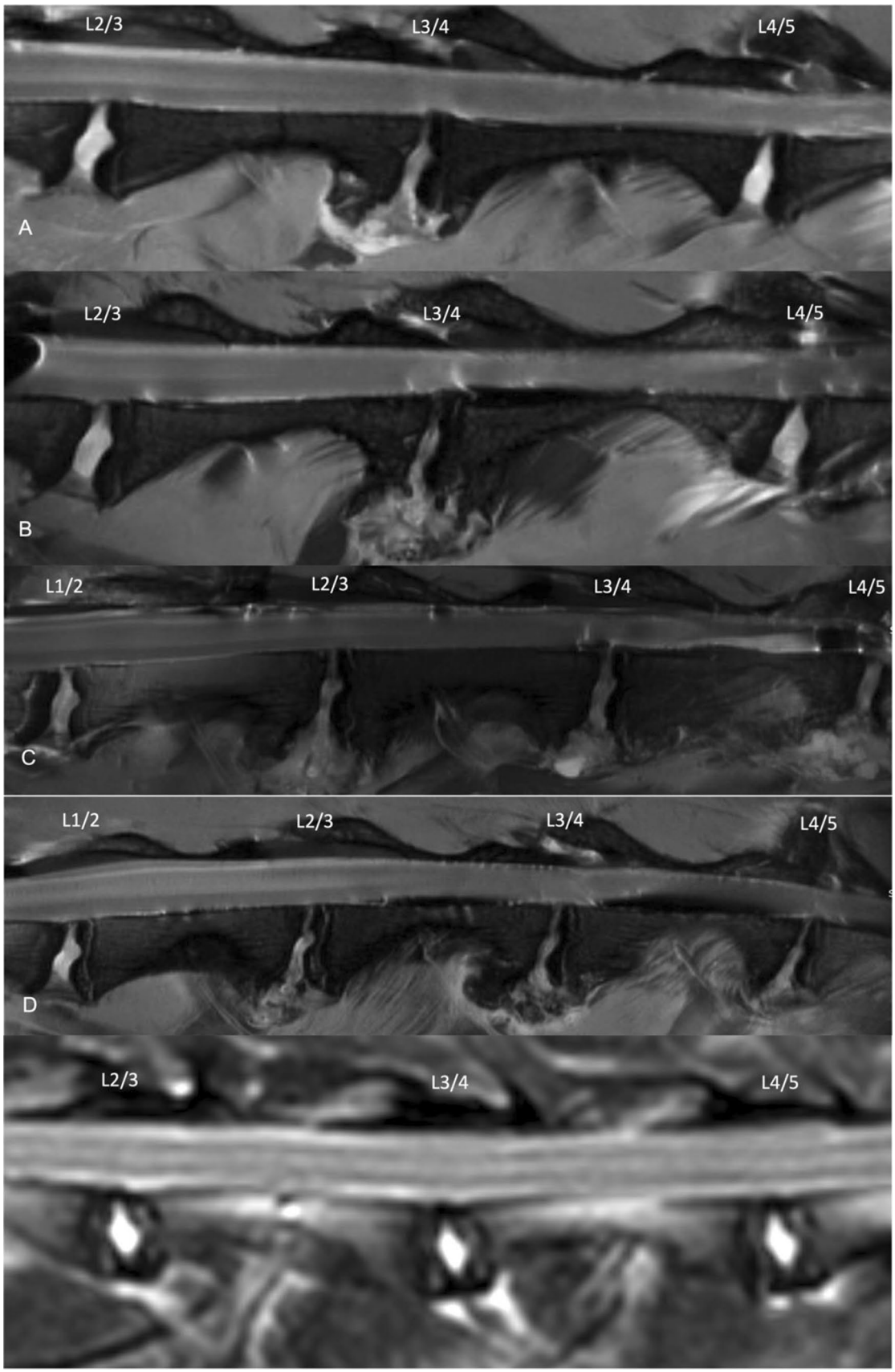
L2/3
L3/4
L4/5
A
L2/3
L3/4
L4/5
B
L1/2
L2/3
L3/4
L4/5
C
L1/2
L2/3
L3/4
L4/5
D
L2/3
L3/4
L4/5

◂**Fig. 6** Representative T2 sagittal μ-MRI sequences of single (**A**, **B**) and multi-level groups (**C**, **D**) at 6 and 12 weeks, respectively, and an age-matched control rabbit (**E**). Note the normal T2 hyperintensity of the NP of the non-operated adjacent and control IVDs, and the loss of this hyperintensity in the fenestrated IVDs

to familiarity with the procedure and appropriate surgeon training. The preclinical model described represents a simple, easy, and safe model of IVDD that would aid research on the aetiology and treatment of IVDD and the effectiveness of many new biomaterial and fusion treatment methods for veterinary and/or human patients.

Fenestration describes the procedure in which the NP is removed by making an incision or window in the AF. Fenestration was originally described in the 1950s as a stand-alone surgical treatment for acute canine IVDE for alleviation of pain and paresis [3, 12, 32, 33]. The rationale for fenestration as a treatment is based on preventing further NP herniation, reduction of the dynamic factors involved in herniation [34], reduction of intradiscal pressure, and elimination of disc-associated pain [35]. In contemporary small animal practice, fenestration is typically performed in combination with decompressive surgery such as hemilaminectomy to remove as much degenerate NP as possible to prevent further extrusion at this site. When performed at the site of disc extrusion, the material remaining within the disc is accessible but the portion that has protruded or extruded, is inaccessible by fenestration alone [19, 36, 37]. Results of large-scale clinical studies evaluating outcome and recurrence after hemilaminectomy with fenestration were summarised by Moore et al. (2020) [38]. The authors identified complications in only 15 (0.01%) patients from more than 1100 cases, and therefore concluded that fenestration is a safe procedure and concern for surgical complication of various types may not be a valid reason for choosing not to fenestrate [38]. Conversely, in a web-based survey of 190 veterinary neurologists and 133 surgeons on the use of concurrent disc fenestration when performing decompressive surgery in the thoracolumbar region, 45% of respondents reported having experienced complications, with haemorrhage being the most common [39]. A further 15% did not feel confident with the technique. There is a paucity of information available in the published literature and clinical practice, on the biological and biomechanical implications of fenestration, particularly for those routinely fenestrating T11- L4.

The complexity of human disc degeneration does not allow any animal model to perfectly mimic the clinical pathophysiological process [25]. A myriad of preclinical animal models of IVDD have been described to mimic the pathobiology of disc degeneration in humans. The model we describe served to induce disc degeneration by fenestration, thereby disrupting the AF and NP, altering the structural integrity of the IVD. Further, the NP removal performed in this study in conjunction with the annular defect may more accurately reflect human spinal pathologies following routine discectomy [40]. Fenestration is akin to microdiscectomy in human medical terms, whereby an annulotomy is performed and the herniated disc material is surgically removed. Indication(s) for microdiscectomy include patients with single-level IVD herniation and evidence of nerve root compression that has residual or unremitting radicular symptoms after failed conservative treatment modalities [41]. Microdiscectomy is a safe and effective treatment for IVDE. Complications from microdiscectomy include iatrogenic injuries such as durotomy, nerve root injury or instability, recurrent disc herniations, haematoma, infection, and persistent pain. One large case series of 2500 microdiscectomy patients reported a complication rate of less than 1.5% [23]; however, like fenestration in veterinary medicine, there is a lack of data on the biological and biomechanical implications of microdiscectomy on the IVD.

In this study, we demonstrated a marked biological consequence of performing lateral lumbar fenestration across multiple endpoint analyses. The gross changes of fibrous tissue on macroscopic dissection were mirrored with the proliferative, spondylotic changes seen on radiography and μCT, sclerotic endplate changes at all treated levels on μCT, and severe IVDD scores on histology. MRI is a common clinical imaging modality used to investigate cases of back pain and evaluate IVD status in human patients [42]. The T2-weighted sequence allows investigation of the anatomical structures and IVD hydration [43]. In this study, T2-weighted sequences allowed visualisation of similar AF and NP morphology changes. Micro-MRI demonstrated marked loss of the normal NP T2 hyperintensity at all treated sites compared to intact IVDs. Quantitative image analysis using Pfirrmann grading, a ranked-based approach to evaluate the severity of IVD degeneration using axial and sagittal T2-weighted MR images [28], further supported the qualitative MRI findings. All AF defects combined with NP removal reliably induced T2 signal changes and generated MR images compatible with IVD degeneration resulting in significantly increased Pfirrmann grading compared to non-operated adjacent and age-matched control IVDs. These changes were seen for all animals through all timepoints and regardless of the order in which the procedures were completed. That is, the 24th rabbit had similar degenerative changes to the first rabbit, independent of the duration of the surgery. This suggests that these changes are acute and lasting. Further, these changes were noted at the disc spaces and not within the surrounding soft tissues, which suggests that the changes seen were related to the surgical insult to the disc space rather than the surgical approach. The translatability of these results to dogs and humans is not without limitations; however, these results may suggest that prophylactic fenestration in canines and microdiscectomy in

Table 2 Pfirrmann μMRI grading IVDD scores of fenestrated and adjacent non-operated control IVDs for single-level and multi-level groups at 6 and 12 weeks ($n=6$ per group per timepoint) and age-matched non-operated control IVDs ($n=6$)

Intervertebral Disc	Grade 1	Grade 2	Grade 3	Grade 4	Grade 5
Single-level group					
L2/3	4/6, 6/6	2/6, –			
L3/4*				0/6, 2/6	6/6, 4/6
L4/5	6/6, 6/6				
Multi-level group					
L1/2	6/6, 6/6				
L2/3*			1/6, 1/6	3/6, 4/6	2/6, 1/6
L3/4*			1/6, 2/6	3/6, 4/6	2/6, –
L4/5*			–, 3/6	6/6, 3/6	
L5/6	6/6, 6/6				
Age-matched control group					
L2/3	6/6				
L3/4	6/6				
L4/5	6/6				

*Fenestrated IVD

humans could have adverse biological responses and fibrous tissue formation. The clinical implications of this in dogs and humans are unknown and are worthy of further study.

The ROM and NZ of fenestrated L3/4 IVD spinal segments were significantly reduced compared to control, non-operated discs in flexion–extension, and lateral bending. The reduced motion is likely due to fibrous tissue formation and ankylosis on the left lateral aspect of the disc space. The 12-week timepoints showed a greater difference compared to the control disc than did the 6-week timepoint, which likely reflects increased deposition and maturation of fibrosis. As defined by Panjabi et al. (1992) [44], the NZ is the portion of the spinal motion load–deflection curve where motion is produced with minimal resistance. The NZ can be more sensitive than range of motion in characterising instability and is a clinically relevant biomechanical metric [45–48]. Additionally, NZ is also commonly measured during biomechanical assessment following disc repair strategies and when characterising material properties [47]. In our study, the NZ, as well as total ROM, was significantly reduced for all fenestrated disc spaces for single-level fenestration compared to controls at both 6- and 12-week timepoints. This result further highlights the biomechanical implications of lateral fenestration of lumbar disc spaces in this model and may help to explain the concept of 'adjacent segment disease' that we see clinically in dogs. In the seminal prospective study by Brisson et al. (2011), the authors reported that 21/24 (87.5%) reoccurrences of IVDE occurred at a disc space immediately adjacent to the previous lesion, at the last site of disc fenestration or 1 disc space away. We postulate that the reason for reoccurrences at these locations is due to ankylosis of the fenestrated disc spaces, which may have reduced the range of motion of that section of thoracolumbar sine, altering spine biomechanics and inducing degeneration at a disc space further cranial or caudal than the typical native herniations. This is speculative, though it is worthy of further investigation in dogs given the findings of our in vivo rabbit model.

Table 3 ROM and NZ for single-level L3/4 fenestration compared to non-operated controls

	Single-level (L3/4)		
	Control (n = 6)	6 weeks (n = 4)	12 weeks (n = 6)
ROM (degrees)			
Lateral Bending	32.15 (1.55)	19.95 (4.35)*	16.16 (2.45)*
Flexion–Extension	25.75 (1.05)	19.46 (2.10)*	17.08 (1.39)*
Axial rotation	4.63 (0.2)	8.05 (1.23)*	6.82 (0.27)
NZ (degrees)			
Lateral Bending	28.63 (1.57)	16.96 (4.84)*	11.27 (1.75)*
Flexion–Extension	18.56 (1.03)	15.41 (1.49)*	12.05 (1.49)*
Axial rotation	1.76 (0.23)	2.82 (0.46)	2.08 (0.39)

Data are presented as mean (standard error)

*Statistically significant compared to controls ($P<0.05$)

A preliminary investigation into the effect of repeated ROM testing of intact rabbit lumbar spinal motion segments confirmed that ROM and NZ were consistent in all planes of motion throughout all repeated tests. Therefore, we can be confident that our observed significant reduction in ROM for fenestrated disc spaces is true. Further, we also previously performed non-destructive robotic ROM testing on cadaveric rabbit vertebral motion segments (L3/4, $n=6$) for intact, annulotomy, and fenestration conditions on the same specimen (unpublished data). Compared to

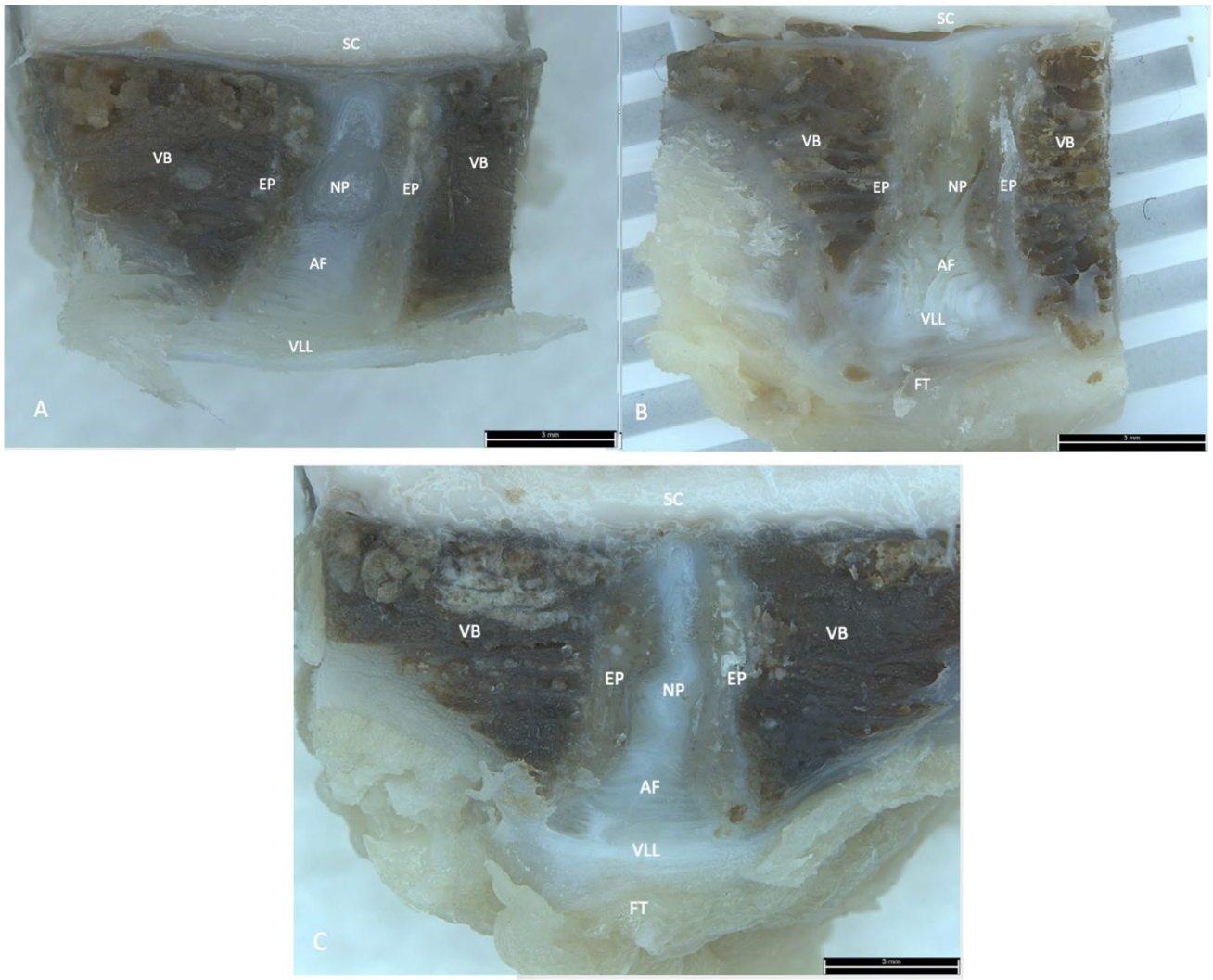

Fig. 7 Stereozoom microscopic appearance in the sagittal plane (1 × objective) of L3/4 IVDs for the following conditions: age-matched non-operated control (**A**), 6 weeks (**B**) and 12 weeks (**C**) post-fenestration. For the fenestrated IVDs (**B**, **C**), note the gross distortion of the IVD architecture, lack of differentiation of the NP from the AF and fibrous tissue formation on the ventral aspect of the disc space (greatest at 12 weeks post-fenestration). Abbreviations: AF Annulus Fibrosus, EP Endplate, FT Fibrous Tissue, NP Nucleus Pulposus, SC Spinal Cord, VB Vertebral Body, VLL Ventral Longitudinal Ligament

intact, fenestrated L3/4 motion segments had significantly increased ROM in all planes of motion ($P = 0.03$) and NZ in flexion–extension ($P = 0.014$). Annulotomy ROM compared to intact approached significance in all planes of motion ($P = 0.07$), while fenestration was not significantly different from annulotomy ($P = 0.41$). It is interesting to note the contrasting result in the present in vivo study, with a significantly reduced ROM for fenestrated IVDs compared to intact. It is likely that ankylosis/fibrosis at the operated site explains this difference, further highlighting the biological implications of the procedure on spine biomechanics. We infer that canine and human patients that undergo fenestration/microdiscectomy also develop a biological response at the fenestrated site and therefore may experience reduced ROM. The ability to detect this clinically and the implications of this on patient outcome need to be further defined.

The severe degenerative macroscopic changes seen on gross examination of sectioned fenestrated disc spaces in conjunction with the significantly greater histological IVDD scores compared to non-operated IVDs, further demonstrates the structural changes induced by lateral fenestration. This may reflect the relevance of this model to mimic severe IVDD in humans and provide a preclinical model for evaluation of treatment strategies in such situations. The histological changes reported (NP and AF morphological disturbance, lamellar disorganisation, decreased cellularity, and EP sclerosis) are consistent with previously described

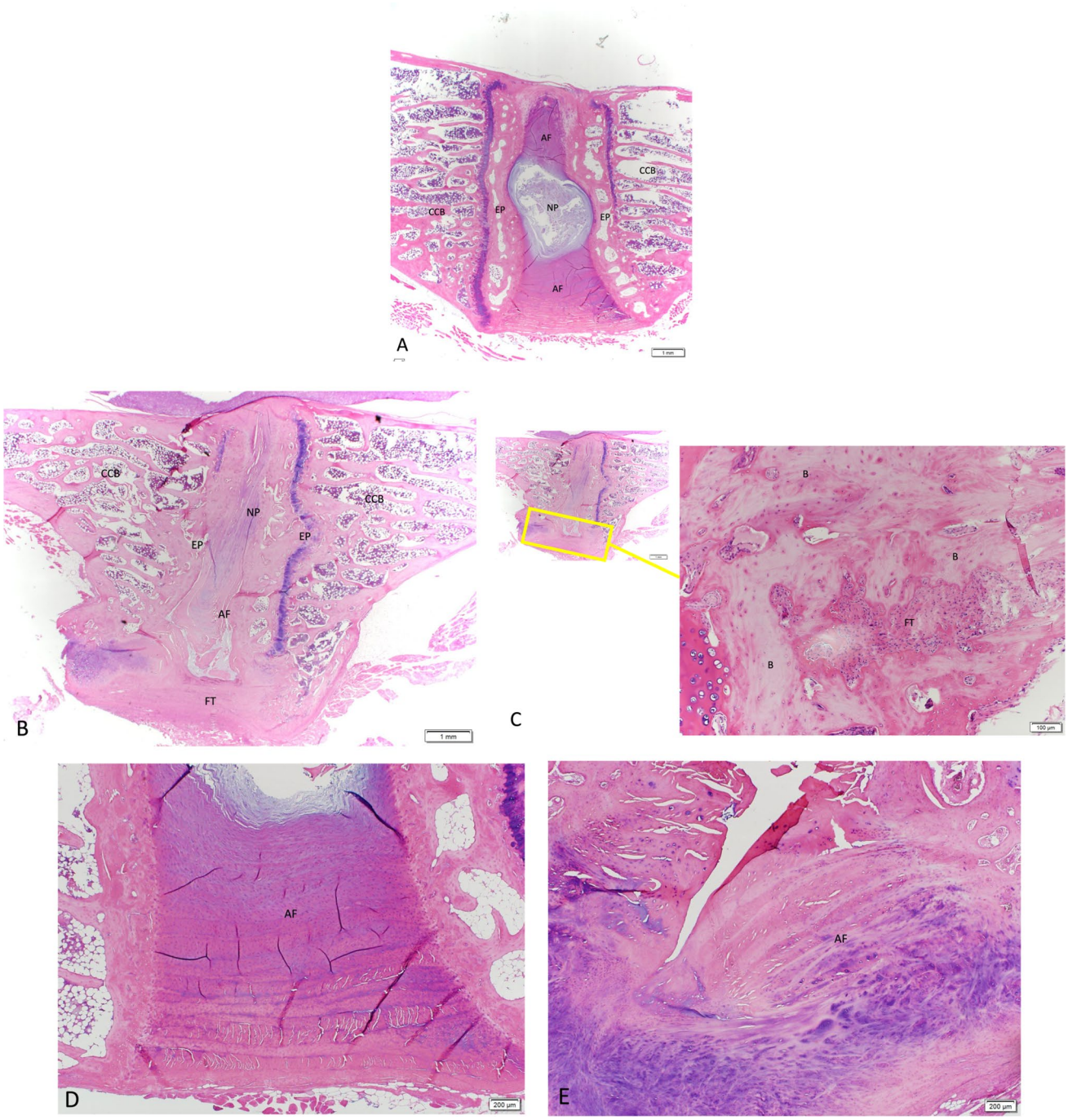

Fig. 8 Haematoxylin and eosin (H&E) stained light-microscopic histopathological images of L3/4 IVDs for the following conditions: age-matched non-operated control (**A**, **D**), and 12 weeks (**B**, **C**, **E**) post-fenestration. For the fenestrated IVDs, note the obliteration of endplate cartilage on the cranial endplate at low magnification (**B**) and under high magnification, amorphous bone formation with interweaving fibrous tissue and mixed inflammatory infiltrates on the ventral aspect of the disc space at 12 weeks post-fenestration (**C**). The control sample shows highly aligned AF lamellae (**D**) compared to disorganised lamellae fibres from a fenestrated IVD 6 weeks postoperative (**E**). Abbreviations: B Bone, AF Annulus Fibrosus, CCB Cancellous Bone, EP Endplate, FT Fibrous Tissue, NP Nucleus Pulposus

Table 4 Total histology grading scores of fenestrated and adjacent non-operated control IVDs for single-level and multi-level groups at 6 and 12 weeks ($n=6$ per group per timepoint) and age-matched non-operated control IVDs ($n=6$)

Intervertebral Disc	Histology Score (0–14)	
	Timepoint	
Single-level group	*6 weeks*	*12 weeks*
L2/3	0.83 (0)	1 (0)
L3/4*	11.66 (0.66)**	11.90 (0.68)**
L4/5	0.5 (0.22)	0.5 (0.22)
Multi-level group		
L1/2	0.83 (0.16)	1 (0)
L2/3*	11.43 (0.56)**	11.28 (0.49)**
L3/4*	11.05 (0.70)**	11.22 (0.72)**
L4/5*	10.88 (0.73)**	11.07 (0.65)**
L5/6	0.66 (0.21)	0.66 (0.21)
Age-matched control group		
L2/3	0 (0)	0 (0)
L3/4	0 (0)	0 (0)
L4/5	0 (0)	0 (0)

Final score (0–14) was totalled from a three-category grading scheme (grade 0–2) across seven evaluated categories: NP morphology (shape and area), NP matrix condensation, NP cellularity, AF/NP border appearance, AF morphology, and endplate (EP) sclerosis/thickening. Data are presented as mean (standard error)

*Fenestrated IVD

**Significantly increased IVDD histological score compared to control IVDs

surgical models of disc degeneration in the rabbit, as well as other species such as mouse, rat, goat, and sheep [25]. Further, SO and PR staining demonstrate reduced proteoglycan and collagen distribution in fenestrated samples compared to controls. The changes observed in this preclinical model are likely more reflective of an acute degenerative process given the 6- and 12-week timepoints used and the severity of the disc degeneration seen histologically. The increase in blood vessel ingrowth and the influx of inflammatory cells was a notable finding and is likely a consequence of the AF injury and a sign for the ongoing degenerative process.

The scoring system used in this study, as described by Gullbrand et al. (2021), was developed based on the prior literature as well as input from spine researchers using the model, and was validated with images across multiple laboratories by 12 independent graders [30]. The use of a single observer to perform the gradings in this study reduced bias between observers given the scoring system has already been validated.

This study was limited in that shorter timepoints prior to 6 weeks and longer timepoints beyond 12 weeks were not examined. Inclusion of these timepoints in future work would provide valuable information on the early biological response and the progressive nature of degeneration, respectively. Additionally, the healthy IVDs of rabbits do not replicate the clinical scenario of pathological chondrodysplastic canine or degenerate human IVDs. Further, the choice of lumbar IVD fenestration may not reflect the thoracolumbar and low lumbar predilection for IVDD in dogs and humans, respectively; however, this location has been used in a myriad of preclinical rabbit models of IVDD and was a more familiar approach for authors. Additionally, rabbits were chosen as preclinical in vivo model species as they more accessible and the use of age- and sex-matched rabbits of known health status from a closed breeding colony allowed for standardisation. Finally, rabbits may have a greater propensity to deposit fibrous tissue compared to dogs and humans. The model described would likely represent acute IVDD rather than a more chronic process, and therefore may not accurately reflect the canine or human chronically diseased state. However, an IVD injury model that produces a short and predictable time course of disc degeneration may allow for targeting a specific timepoint and reduce the cost concerns of regenerative therapy studies [42].

Conclusions

This study describes an in vivo preclinical rabbit model of lateral fenestration of lumbar IVDs that demonstrates the medium-term biological and biomechanical implications of fenestration and microdiscectomy. The technique may represent a suitable preclinical model to evaluate new IVDD treatment strategies for veterinary and human patients. Veterinary and human spine surgeons should consider the biological and biomechanical implication of their surgical technique, especially when performed prophylactically, and balance this against the perceived benefits of surgery.

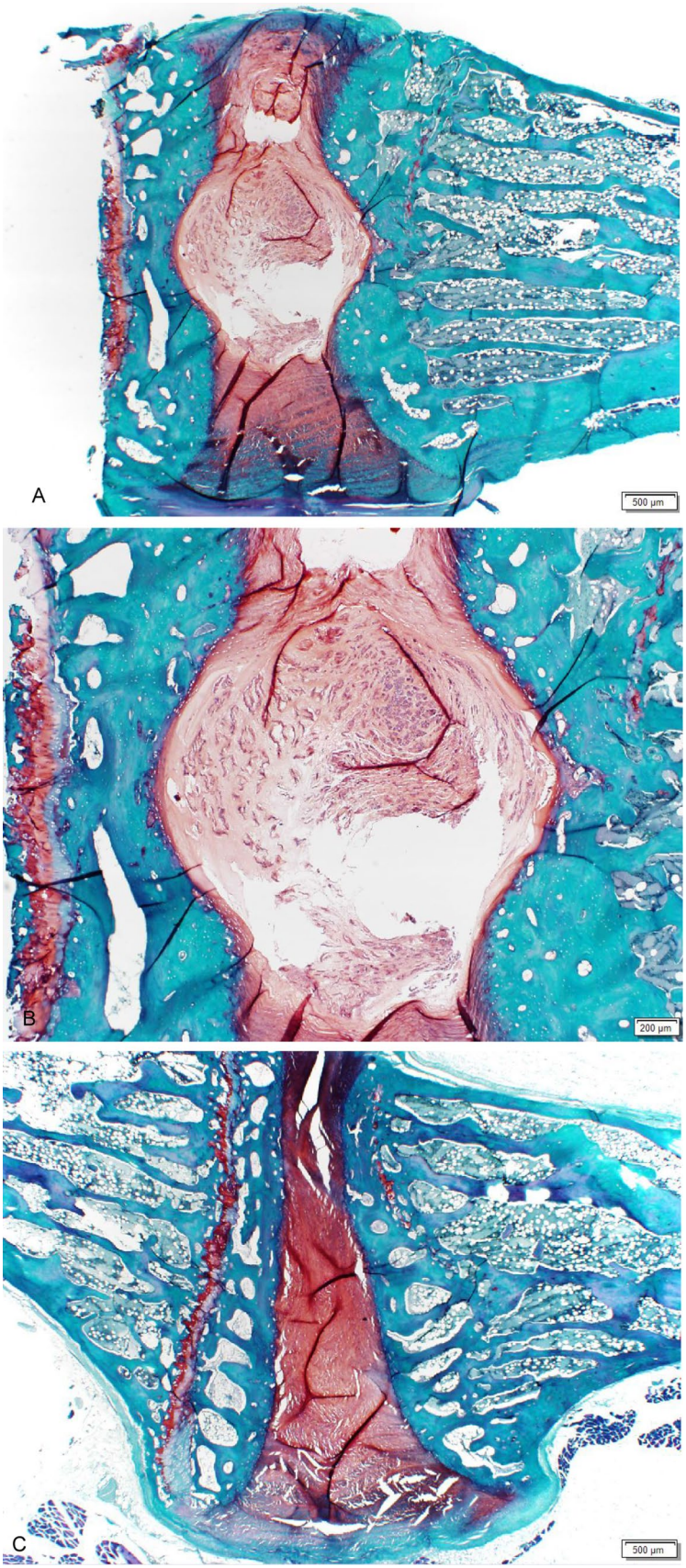

Fig. 9 Safranin-O (SO) stained light-microscopic histopathological images of L3/4 IVDs for the following conditions: adjacent non-operated control (L2/3) (**A**, **B**) and L3/4 disc 12 weeks post-fenestration (**C**). For the fenestrated IVDs, note the collapse of the disc space and intense, denser staining of proteoglycan content remaining in the disc space. For non-operated control discs at low and higher power (**A**, **B**), note the concavity of the nucleus pulposus, and the central, gelatinous NP with cellular content, and less densely staining, proteoglycan rich content scattered throughout the NP. Abbreviations: AF Annulus Fibrosus, CCB, Cancellous Bone, EP Endplate, NP Nucleus Pulposus

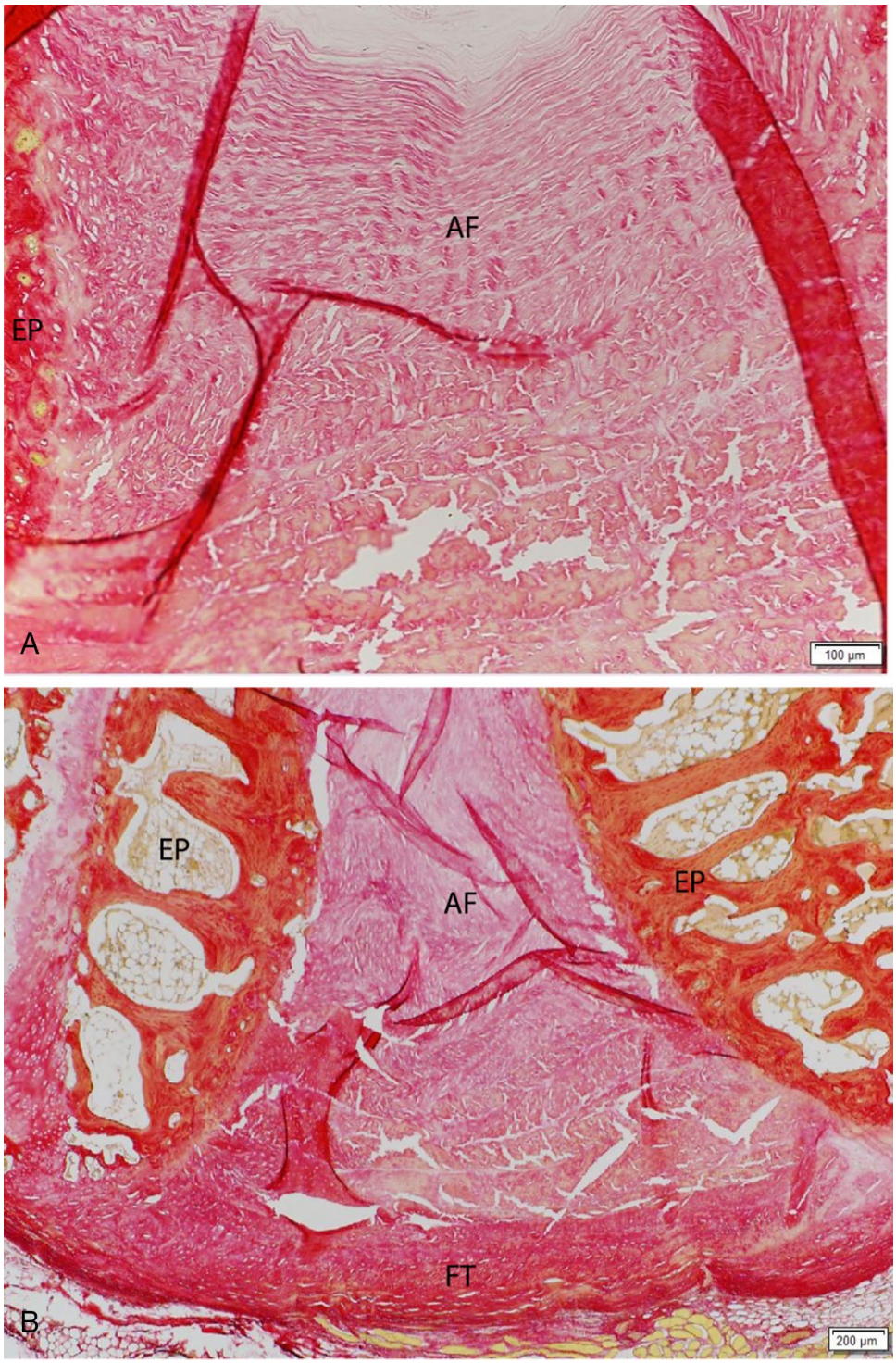

Fig. 10 Picrosirius red (PR) stained light-microscopic histopathological images of L3/4 IVDs for the following conditions: adjacent non-operated control (L2/3) (**A**) and L3/4 disc 12 weeks post-fenestration (**B**). For the control disc, note the concentric, organised arrangement of lamellar collagen fibres on the ventral aspect of the disc space. For the fenestrated disc, note the disorganisation and disruption of the lamellar fibres. Abbreviations: AF Annulus Fibrosus, EP Endplate, FT Fibrous Tissue

Acknowledgements The authors acknowledge the facilities and scientific support by Brendan Lee and Dr Andre Bongers at the Biological Research Imaging Laboratory (BRIL), UNSW, Sydney node of the National Imaging Facility, a National Collaborative Research Infrastructure Strategy (NCRIS) capability. The authors thank Marcus Cremonese for his schematic illustrations.

Author contributions All authors provided substantial contributions to research design, acquisition, analysis, and interpretation of the current literature. Rema Oliver and Tian Wang were involved in data collection, data analysis, and manuscript review. Matthew Pelletier contributed to study design and manuscript review. James Crowley was involved in data collection, data analysis, and drafted the manuscript.

William Walsh contributed to study design, concept development, and manuscript review. All authors have read and revised the whole manuscript critically and approved the final submitted version.

Funding Open Access funding enabled and organized by CAUL and its Member Institutions.

Declarations

Conflict of interest None of the authors has any potential conflict of interest.

References

1. Dan MJ, Crowley J, Broe D, Cross M, Tan C, Walsh WR (2019) Patella tendinopathy Zoobiquity—What can we learn from dogs? Knee 26:115–123
2. Jeffery ND, Freeman PM (2018) The role of fenestration in management of type I thoracolumbar disk degeneration. Vet Clin: Small Anim Pract 48:187–200
3. Freeman P, Jeffery N (2017) Re-opening the window on fenestration as a treatment for acute thoracolumbar intervertebral disc herniation in dogs. J Small Anim Pract 58:199–204
4. Hamawandi SA, Sulaiman II, Al-Humairi AK (2020) Open fenestration discectomy versus microscopic fenestration discectomy for lumbar disc herniation: a randomized controlled trial. BMC Musculoskelet Disord 21:1–11
5. Brisson BA, Holmberg DL, Parent J, Sears WC, Wick SE (2011) Comparison of the effect of single-site and multiple-site disk fenestration on the rate of recurrence of thoracolumbar intervertebral disk herniation in dogs. J Am Vet Med Assoc 238:1593–1600
6. Forterre F, Konar M, Spreng D, Jaggy A, Lang J (2008) Influence of intervertebral disc fenestration at the herniation site in association with hemilaminectomy on recurrence in chondrodystrophic dogs with thoracolumbar disc disease: a prospective MRI study. Vet Surg 37:399–405
7. Mayhew PD, McLear RC, Ziemer LS, Culp WT, Russell KN, Shofer FS, Kapatkin AS, Smith GK (2004) Risk factors for recurrence of clinical signs associated with thoracolumbar intervertebral disk herniation in dogs: 229 cases (1994–2000). J Am Vet Med Assoc 225:1231–1236
8. Aikawa T, Fujita H, Shibata M, Takahashi T (2012) Recurrent thoracolumbar intervertebral disc extrusion after hemilaminectomy and concomitant prophylactic fenestration in 662 chondrodystrophic dogs. Vet Surg 41:381–390
9. Aikawa T, Fujita H, Kanazono S, Shibata M, Yoshigae Y (2012) Long-term neurologic outcome of hemilaminectomy and disk fenestration for treatment of dogs with thoracolumbar intervertebral disk herniation: 831 cases (2000–2007). J Am Vet Med Assoc 241:1617–1626
10. Brisson BA, Moffatt SL, Swayne SL, Parent JM (2004) Recurrence of thoracolumbar intervertebral disk extrusion in chondrodystrophic dogs after surgical decompression with or without prophylactic enestration: 265 cases (1995–1999). J Am Vet Med Assoc 224:1808–1814
11. Funkquist B (1978) Investigations of the therapeutic and prophylactic effects of disc evacuation in cases of thoraco-lumbar herniated discs in dogs. Acta Vet Scand 19:441–457
12. Butterworth S, Denny H (1991) Follow-up study of 100 cases with thoracolumbar disc protrusions treated by lateral fenestration. J Small Anim Pract 32:443–447
13. Davies J, Sharp N (1983) A comparison of conservative treatment and fenestration for thoracolumbar intervertebral disc disease in the dog. J Small Anim Pract 24:721–729
14. Levine S, Caywood D (1984) Recurrence of neurological deficits in dogs treated for thoracolumbar disk disease. J Am Anim Hosp Assoc (USA)
15. Black A (1988) Lateral spinal decompression in the dog: a review of 39 cases. J Small Anim Pract 29:581–588
16. Knapp D, Pope E, Hewett J, Bojrab M (1990) A retrospective study of thoracolumbar disk fenestration in dogs using a ventral approach: 160 cases (1976 to 1986). J Am Anim Hosp Assoc 26:543–549
17. Scott H (1997) Hemilaminectomy for the treatment of thoracolumbar disc disease in the dog: a follow-uo studv of 40 cases. J Small Anim Pract 38:488–494
18. Dhupa S, Glickman N, Waters DJ (1999) Reoperative neurosurgery in dogs with thoracolumbar disc disease. Vet Surg 28:421–428
19. Brown N (1977) Thoracolumbar disk disease in the dog. A retrospective analysis of 187 cases. J Am Anim Hosp Assoc 13:665–672
20. Nečas A (1999) Clinical aspects of surgical treatment of thoracolumbar disc disease in dogs. A retrospective study of 300 cases. Acta Vet Brno 68:121–130
21. Prata R (1981) Neurosurgical treatment of thoracolumbar disks: the rationale and value of laminectomy with concomitant disk removal. J Am Anim Hosp Assoc (USA)
22. Tullberg T, Isacson J, Weidenhielm L (1993) Does microscopic removal of lumbar disc herniation lead to better results than the standard procedure? Results of a one-year randomized study. Spine 18:24–27
23. Koebbe CJ, Maroon JC, Abla A, El-Kadi H, Bost J (2002) Lumbar microdiscectomy: a historical perspective and current technical considerations. Neurosurg Focus 13:1–6
24. Daly C, Ghosh P, Jenkin G, Oehme D, Goldschlager T (2016) A review of animal models of intervertebral disc degeneration: pathophysiology, regeneration, and translation to the clinic. BioMed Res Int 2016
25. Poletto DL, Crowley JD, Tanglay O, Walsh WR, Pelletier MH (2023) Preclinical in vivo animal models of intervertebral disc degeneration. Part 1: a systematic review. JOR Spine 6:e1234
26. Crowley JD, Oliver RA, Dan MJ, Wills DJ, Rawlinson JW, Crasto RA, O'Connor JM, Mitchell GJ, Tan CJ, Walsh WR (2021) Single level posterolateral lumbar fusion in a New Zealand White rabbit (Oryctolagus cuniculus) model: surgical anatomy, operative technique, autograft fusion rates, and perioperative care. JOR Spine 4:e1135
27. Lü D-S, Shono Y, Oda I, Abumi K, Kaneda K (1997) Effects of chondroitinase ABC and chymopapain on spinal motion segment biomechanics. An in vivo: biomechanical, radiologic, and histologic canine study. Spine 22:1828–1834

28. Pfirrmann CW, Metzdorf A, Zanetti M, Hodler J, Boos N (2001) Magnetic resonance classification of lumbar intervertebral disc degeneration. Spine 26:1873–1878
29. Conway JC, Oliver RA, Wang T, Wills DJ, Herbert J, Buckland T, Walsh WR, Gibson IR (2021) The efficacy of a nanosynthetic bone graft substitute as a bone graft extender in rabbit posterolateral fusion. Spine J 21:1925–1937
30. Gullbrand SE, Ashinsky BG, Lai A, Gansau J, Crowley J, Cunha C, Engiles JB, Fusellier M, Muehleman C, Pelletier M (2021) Development of a standardized histopathology scoring system for intervertebral disc degeneration and regeneration in rabbit models-An initiative of the ORS spine section. JOR Spine 4:e1147
31. Lee NN, Kramer JS, Stoker AM, Bozynski CC, Cook CR, Stannard JT, Choma TJ, Cook JL (2020) Canine models of spine disorders. JOR Spine 3:e1109
32. Flo G, Brinker W (1975) Lateral fenestration of thoracolumbar discs [Surgery, dogs]. J Am Anim Hosp Assoc
33. Denny H (1978) The lateral fenestration of canine thoracolumbar disc protrusions: a review of 30 cases. J Small Anim Pract 19:259–266
34. Olsson S-E (1951) Observations concerning disc fenestration in dogs. Acta Orthop Scand 20:349–356
35. Butterworth SJ, Kydd DM (2017) TTA-Rapid in the treatment of the canine cruciate deficient stifle: short- and medium-term outcome. J Small Anim Pract 58:35–41. https://doi.org/10.1111/jsap.12610
36. Hill T, Lubbe A, Guthrie A (2000) Lumbar spine stability following hemilaminectomy, pediculectomy, and fenestration. Vet Comp Orthop Traumatol 13:165–171
37. Fingeroth J (1989) Fenestration. Pros and cons. Probl Vet Med 1:445–466
38. Moore SA, Tipold A, Olby NJ, Stein V, Granger N, Injury CSC (2020) Current approaches to the management of acute thoracolumbar disc extrusion in dogs. Front Vet Sci 7:610
39. Hall JF, Freeman P (2021) Approach to and practice of disc fenestration in the management of intervertebral disc extrusions in dogs: a questionnaire survey. Vet Comp Orthop Traumatol 34:437–440
40. Klassen PD, Hsu WK, Martens F, Inzana JA, van den Brink WA, Groff MW, Thomé C (2018) Post-lumbar discectomy reoperations that are associated with poor clinical and socioeconomic outcomes can be reduced through use of a novel annular closure device: results from a 2-year randomized controlled trial. ClinicoEcon Outcomes Res 349–357
41. Burke J, Watson R, McCormack D, Dowling F, Walsh M, Fitzpatrick J (2002) Intervertebral discs which cause low back pain secrete high levels of proinflammatory mediators. J Bone Joint Surg Br 84:196–201
42. Constant C, Hom WW, Nehrbass D, Carmel EN, Albers CE, Deml MC, Gehweiler D, Lee Y, Hecht A, Grad S (2022) Comparison and optimization of sheep in vivo intervertebral disc injury model. JOR Spine 5:e1198
43. Gold GE, Han E, Stainsby J, Wright G, Brittain J, Beaulieu C (2004) Musculoskeletal MRI at 3.0 T: relaxation times and image contrast. Am J Roentgenol 183:343–351
44. Panjabi MM (1992) The stabilizing system of the spine. Part II. Neutral zone and instability hypothesis. Clin Spine Surg 5:390–397
45. Panjabi MM (1992) The stabilizing system of the spine. Part I. Function, dysfunction, adaptation, and enhancement. J Spinal Disord 5:383–383
46. Wilke H-J, Wenger K, Claes L (1998) Testing criteria for spinal implants: recommendations for the standardization of in vitro stability testing of spinal implants. Eur Spine J 7:148–154
47. Panjabi MM (2003) Clinical spinal instability and low back pain. J Electromyogr Kinesiol 13:371–379
48. Volkheimer D, Galbusera F, Liebsch C, Schlegel S, Rohlmann F, Kleiner S, Wilke H-J (2018) Is intervertebral disc degeneration related to segmental instability? An evaluation with two different grading systems based on clinical imaging. Acta Radiol 59:327–335